



Analyses of Diamond - Shaped and Circular Arc Airfoils in Supersonic Wind Tunnel Airflows

Modo U. P, Chukwunke J. L, Omenyi Sam

¹Department of Mechanical Engineering, Nnamdi Azikiwe University, Awka, Nigeria

ABSTRACT

In this research, the lift force produced by a diamond shaped airfoil and Circular arc airfoil under flight condition were discussed. The diamond shaped airfoil and circular arc airfoil were tested in a supersonic wind tunnel. The diamond shaped airfoil having a weight of 71N and a wing area of 0.014m² and Circular arc airfoil having a weight of 96N and a wing area of 0.014m² were analyzed. These airfoils were experimentally tested in a supersonic wind tunnel at Mach 1.8 and at angle of attack of 30° to airflow. A load having a weight of 30N was placed on the mass scale during testing. It was found that at 30° angle of attack to airflow, the diamond shaped airfoil produced a lift force of 11N and 10N for first and second testing respectively while circular arc airfoil produced a lift force of 6N and 5N for first and second testing respectively at Mach number of 1.8. The pressure and temperature distributions on the surfaces of a diamond shaped airfoil under flight condition were discussed and the diamond shaped airfoil was analyzed using linear theory. An airplane of diamond shaped airfoil having a weight of 140000N and a wing area of 28m² was analyzed at a given altitude of 13000m. The lift and drag coefficients of the diamond shaped airfoil were calculated as function of Mach numbers from M=1.4 to M=2.8. Maximum lift coefficient and drag coefficient were found to be 0.22288 and 0.02237 respectively at Mach number of 1.4 while minimum lift coefficient and wave drag coefficient were found to be 0.05572 and 0.00585 respectively at Mach number of 2.8. Maximum pressure and temperature were found on surface 3 of the diamond shaped airfoil with values of 21333.42N/m² and 219.71K respectively at Mach number of 1.8 which gave the maximum lift to drag ratio of 10. Minimum pressure and temperature were found on surface 2 of the diamond shaped airfoil with values of 11377.78N/m² and 183.59K respectively at Mach number of 1.8 which gave the maximum lift to drag ratio of 10. Linear theory software for airfoil was developed to handle all the numerical computation that was done.

Keywords- Aerodynamic, Airfoil, Angle of Attack, Lift and Drag Coefficient, Linear theory, Mach number, Surface, Temperature and Pressure Distribution, Wind Tunnel.

1. INTRODUCTION

The shape of the airfoil is what determines the pressure distribution around the airfoil thereby determining the lift and drag forces generated. This means that accurate construction of the wing (airfoil) is of paramount as error or poor construction will affect the aerodynamic performance of the wing of the aircraft because most airfoils have camber and curved surfaces and these curved surfaces pose serious problem to airfoil designers during construction. This problem associated with accurate construction of curved surfaces will be eliminated by the diamond shaped airfoil because it has no camber and curved surfaces.

The wings of aircraft are designed using airfoil shapes because an airfoil-shaped body moving through a fluid is subjected to an aerodynamic force. Lift is the component of this force perpendicular to

the direction of motion and drag is the component parallel to the direction of motion (PrabhakaraRao and Sampath, 2014). Most airfoil shapes require a positive angle of attack for lift to be generated but at zero angle of attack the lift is generated on cambered airfoils (Houghton and Carpenter, 2003). Primarily, the result of its angle of attack and shape is due to the lift on an airfoil. The airfoil deflects the oncoming air when oriented at a suitable angle, resulting in a force (aerodynamic force) on the airfoil in the direction opposite to the deflection. This revolving of the air in the surrounding area of the airfoil generates curved streamlines resulting in higher pressure on one side and lower pressure on the other (PrabhakaraRao and Sampath, 2014). This pressure difference goes with a velocity difference by means of Bernoulli's principle, so the resulting flow field about the airfoil has a



higher average velocity on the upper surface than on the lower surface (Bruschi, et al 2003; Cavcar, 2003). The concept of circulation and the Kutta-Joukowski theorem can relate the lift force directly to the average top/bottom velocity difference without computing the pressure (Anderson, 2001).

The thickness ratio of an airfoil is a parameter which is usually specified and the effect of thickness of an airfoil is to increase the lift coefficient (C_L). Increasing the camber and thickness beyond a certain limit will make the body to depart from being a streamlined body to being a bluff body; separation of flow will occur and wake will be formed which will destroy lift as a result (Bertin and Cummings, 2009). The primary purpose of an airfoil is to produce lift when placed in a fluid stream which of course experience drag at the same time. In an aircraft, lift on the wing surfaces maintains the aircraft in the air and drag absorbs all the engine power necessary for forward motion of the craft (Karabelas and Markatos, 2008). In order to minimize drag, an airfoil is a streamlined body. The ratio of lift to drag gives a measure of the usefulness of an airfoil as a wing section of an aircraft. The higher this ratio the better the airfoil since it is capable of producing high lift at a small drag penalty (Douglas, 2000). The ratio of lift to drag is expressed as L/D ratio or C_L/C_D ratio and can be determined by flight test in a wind tunnel. If this ratio is high, then the airfoil can be used to produce useful lift which makes the aircraft to fly (Salem and Ibrahim, 2004). An aircraft has a high L/D ratio or C_L/C_D ratio if it produces a large amount of lift or a small amount of drag.

Furthermore, the numerical computation of the equations in linear theory is tedious and could pose a problem to airfoil designers and analyst. However, linear theory software for airfoil has been developed to solve this problem. This linear theory software for airfoil can calculate faster and accurately all

parameters in linear theory equations and display their results. This research compared and analyzed the diamond shaped airfoil and circular arc airfoil under flight conditions. The diamond shaped airfoil and circular arc airfoil were tested in a supersonic wind tunnel.

2. METHODOLOGY

2.1 Theoretical Considerations- Linear Theory

The linear theory is an approximation theory assuming small perturbations (that is, the hump is small and the angle of inclination to free stream, θ , is small). The linear theory can be used for supersonic speeds only rather than transonic or hypersonic. The linear theory is very useful for estimating the lift and wave drag of supersonic airfoils. The lift coefficient decreased with increasing Mach numbers as linear theory predicts by their inverse relationship. Similarly, the drag coefficient decreased with increasing Mach numbers as linear theory predicts by their inverse relationship. It is an interesting fact that when the surface is inclined into the free stream direction, linear theory predicts a positive C_p . In contrast, when the surface is inclined away from the free stream direction, linear theory predicts a negative C_p . In other words, deflection angle, θ , is positive when the flow is being turned away from the free stream direction and negative when the flow is being turned back. The diamond shaped airfoil (see figure 1) and Circular arc airfoil (see figure 2) have four surfaces namely surface 1, surface 2, surface 3 and surface 4. Surface 1 and surface 3 are inclined into the free stream; therefore C_{p1} and C_{p3} are positive values. In contrast, surface 2 and surface 4 are inclined away from the free stream, therefore C_{p2} and C_{p4} are negative values.

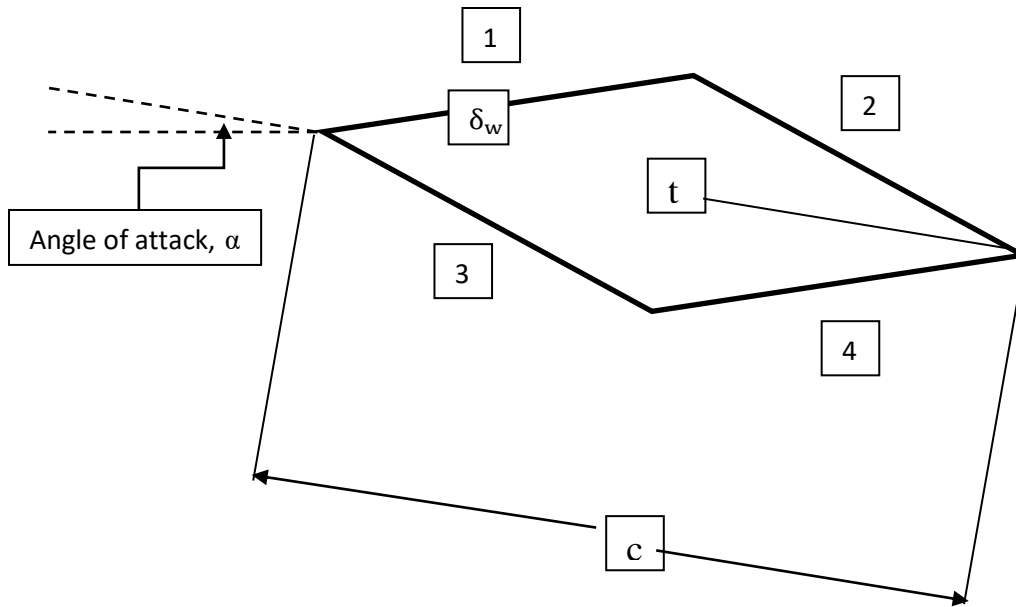


Figure 1: Symmetric diamond shaped airfoil.

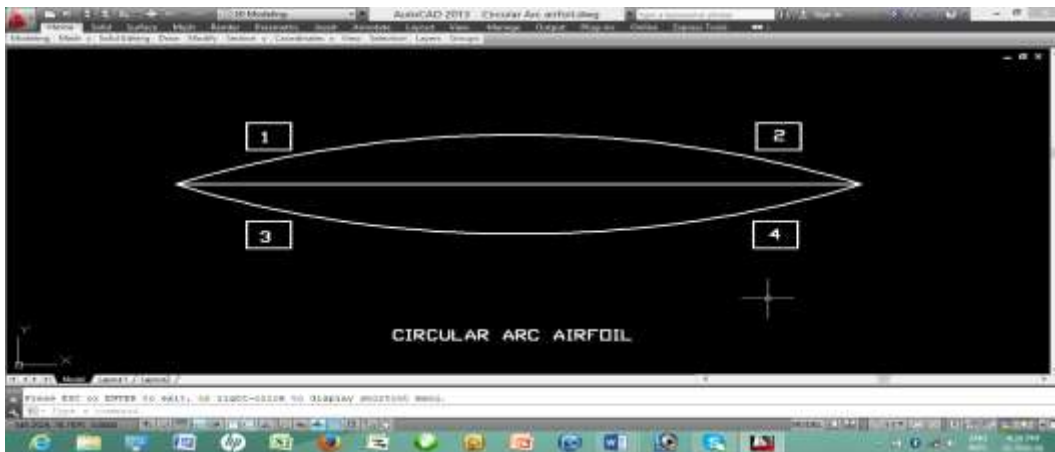


Figure 2: Symmetric Circular Arc airfoil.

II Linear Theory for Diamond Shaped Airfoil

The dynamic pressure is given by (Douglas, 2000):

$$q = \frac{1}{2} \rho V^2 \quad (1)$$

Where: q = dynamic pressure, ρ = fluid density and V = fluid velocity.

If the fluid in question is considered as an ideal gas, then the dynamic pressure can be expressed as a function of fluid density, ρ , and Mach number, Ma , by applying the ideal gas law:

$$P = \rho R_s T \quad (2)$$

Where: P = fluid pressure, R_s = Specific gas constant and T = temperature of the gas/air.

The speed of sound in air is given:

$$a = \sqrt{\gamma R_s T} \quad (3)$$

Where: a = speed of sound and γ = Specific heat of air.

The expression for speed of sound states that the speed of sound in a calorically perfect gas is a function of temperature only. The Mach number is given by (Anderson, 2001):

$$Ma = \frac{V}{a} \quad (4)$$

Substituting equations (3) and (4) into equation (1), the dynamic pressure is expressed as a function of



fluid density, ρ and Mach number, Ma as shown in equation (5):

$$q = \frac{1}{2} \rho (Ma \sqrt{\gamma R_s T})^2 \quad (5)$$

For free stream conditions, equation (5) can then be expressed as:

$$q_\infty = \frac{1}{2} \rho_\infty (M_\infty \sqrt{\gamma_{air} R_s T_\infty})^2 \quad (6)$$

The lift coefficient can be calculated using (Anderson, 2001):

$$C_L = \frac{W}{(q_\infty A)} \quad (7)$$

The angle of attack is calculated using (Anderson, 2001):

$$\alpha = \frac{C_L \sqrt{(M_\infty^2 - 1)}}{4} \quad (8)$$

The drag coefficient is calculated using (Auld and Srinivas, 2010):

$$C_D = \frac{4\alpha^2}{\sqrt{(M_\infty^2 - 1)}} + \frac{2}{\sqrt{(M_\infty^2 - 1)}} \int_0^1 \left[\left(\frac{dy_u}{dx} \right)^2 + \left(\frac{dy_L}{dx} \right)^2 \right] d\left(\frac{x}{c}\right) + \frac{4}{\sqrt{(M_\infty^2 - 1)}} \int_0^1 k d\left(\frac{x}{c}\right) \quad (9)$$

Where: $\frac{x}{c}$ ranges from 0 at the leading edge to 1 at the trailing edge, ($0 \leq \frac{x}{c} \leq 1$), $\frac{dy_u}{dx} = \tan \delta_w = \frac{t}{c}$ and $\frac{dy_L}{dx} = -\tan \delta_w = -\frac{t}{c}$, $k = 0$ for a symmetric airfoil (zero camber).

The lift to drag ratio can be calculated using (Douglas, 2000):

$$\frac{\text{Lift}}{\text{Drag}} = \frac{1/2 \rho C_L U_\infty^2 A}{1/2 \rho C_D U_\infty^2 A} = \frac{C_L}{C_D} \quad (10)$$

The deflection angle θ_j for the corresponding surface j of the airfoil is given by equation (11)

$$\theta_j = \frac{dy_j}{dx} - \alpha_j \quad (11)$$

The pressure coefficient for each surface j of the airfoil is calculated using [Anderson, 2001]:

$$C_{p_j} = \frac{2\theta_j}{\sqrt{(M_\infty^2 - 1)}} \quad (12)$$

The pressure P_j of each surface j of the airfoil is calculated using (Anderson, 2001):

$$P_j = (C_{p_j} \times q_\infty) + P_\infty \quad (13)$$

Since the flow is isentropic, temperature T_j of each surface j of the airfoil is related to pressure P_j by:

$$T_j = T_\infty \left[\frac{P_j}{P_\infty} \right]^{\frac{\gamma-1}{\gamma}} \quad (14)$$

2.2 Supersonic Wind Tunnel

A supersonic wind tunnel was constructed (see figure 3) for the experimental setup. A supersonic wind tunnel is a wind tunnel that produces supersonic speeds ($1.2 < Ma < 5$). The supersonic wind tunnel used for this research was for Mach number 1.8. A convergent – divergent nozzle feeds a uniform

Convergent divergent nozzle: The convergent-divergent nozzle has two ends. One End is open to the atmosphere for air intake while the other end is attached to the test section. The convergent-divergent nozzle is made from iron sheets and has the

supersonic flow into the constant – area duct, which is called the test section. This flow is subsequently slowed to a low subsonic speed by means of a diffuser. The supersonic wind tunnel consists of the following: Convergent-divergent nozzle, Test section, Convergent-divergent diffuser and Support stand

smallest area of the wind tunnel which is called nozzle throat area or sonic throat area. Pressure difference must be created between the inlet and exit of the nozzle, only then will the air start to flow through the nozzle. The exit pressure must be less than the inlet pressure.



Figure 3: Picture of Indraft Supersonic Wind Tunnel

Test Section: The test section, for Mach number of 1.8, has two ends. One End is connected to the convergent-divergent nozzle while the other end is attached to the convergent divergent diffuser. The test section is made from Perspex glass and has the largest area of the wind tunnel. The test section is where the airfoil is placed for testing and must be airtight as much as possible. A test model such as airfoil is placed in the test section where aerodynamic measurement such as lift is made. The test model (airfoil) is suspended in the test section by means of strings. A controlling device for controlling the angle of attack of airfoil to airflow is mounted on the test section. A string is also used to connect the airfoil to a load placed on the mass scale.

Convergent-divergent diffuser: The convergent-divergent diffuser has two ends. One End is connected to the test section while the other end houses the fan section. The convergent-divergent diffuser is made from plywood and has an area which is called diffuser throat area. The diffuser throat area must always be larger than the nozzle throat area. If the diffuser throat area is less than the nozzle throat area, the diffuser will choke, meaning that the diffuser cannot pass the mass flow coming from the isentropic supersonic expansion through the nozzle.

Support Stand: The support stand provides a platform upon which the wind tunnel is placed. The support stand is made from iron pipes which can be assembled and disassembled for ease of mobility. The support stand also provides a platform upon which the mass scale is placed. The mass scale tells the mass or weight of the load placed on it before and during the period of time that the wind tunnel is in operation.

2.3 Wind Tunnel Parameters

The supersonic wind tunnel used for this research was constructed for Mach number 1.8 as required in the test section. Using Mach number of 1.8 and specific heat of air (γ) of 1.4, the area ratio A/A^* was calculated to be 1.439. The dimension of the test section is chosen to be 200mm by 200mm by 300mm. The area of the test section (A) is 40000mm² and the sonic throat area (A^*) is calculated to be 27777.77mm². The convergent-divergent nozzle has a length of 300mm.

From the normal shock properties table, at Mach number of 1.8, $\frac{P_{0,2}}{P_{0,1}}$ is found to be 0.8127:

$$\frac{A_{t,2}}{A_{t,1}} = \frac{P_{0,1}}{P_{0,2}} \quad (15)$$

Where: $A_{t,1}$ = Nozzle throat area or sonic throat area, $A_{t,2}$ = Diffuser throat area, $P_{0,1}$ = Pressure at inlet to nozzle and $P_{0,2}$ = Pressure at exit of nozzle.

From equation (15), the diffuser throat area, $A_{t,2}$ is calculated to be 34179.61mm². The convergent-divergent diffuser has a length of 500mm. The wind speed in the test section can be determined mathematically using equation (4). Using a Mach number of 1.8 and a speed of sound of 343.11m/s at room temperature of 20°C together with equation (4), the wind speed is calculated to be 617.59m/s.

The volumetric flow rate of the fan required can also be determined mathematically:

$$V = \frac{Q}{A} \quad (16)$$

Where: V = Wind speed, Q = Volumetric flow rate and A = Flow cross section area.

Using a wind speed of 617.59m/s and cross section area of 0.04m² together with equation (16), the volumetric flow rate is calculated to be 24.7m³/s. The fan required for the tunnel should have a volumetric

$$T=T_o - (L \times h) \tag{17}$$

$$P=P_o \left(1 - \frac{L \times h}{T_o}\right)^{\frac{g \times M}{R \times L}} \tag{18}$$

$$\rho = \frac{P \times M}{R \times T} \tag{19}$$

2.4 Experimentation

The experimental set-up is shown in figure 3 and a sketch on how the airfoil is connected to the angle of attack controlling device and load is shown in figure 4. The mass or weight of diamond shaped airfoil; circular arc airfoil and load are taken and recorded. The convergent-divergent nozzle will be at the forward end of the wind tunnel into which the air will flow as it is drawn in by the fan at the back. The test section is between the convergent-divergent nozzle and convergent-divergent diffuser. The convergent divergent diffuser will be at the back end of the wind tunnel and it houses the fan. The fan will blow out of the wind tunnel, not into it, which is why the fan is at the back end of the wind tunnel. The test model (airfoil) is placed in the test section. Strings from the angle of attack controlling device and from the top of the test section are connected to the airfoil while another string passing through a hole at the bottom of the test section connects the diamond shaped airfoil to the load which is placed on the mass scale. The angle of attack controlling device is used to place the diamond shaped airfoil at angle 30° of attack to

flow rate of 24.7m³/s or 52336.1 CFM. Temperature, pressure and density at altitude h meters above sea level are given by (Anderson, 2001):

airflow and the window of the tunnel is closed. The weight of the load connected to the airfoil at angle 30° of attack is recorded before the wind tunnel is started. As the fan draws in air through the wind tunnel, the diamond shaped airfoil at angle 30° of attack to airflow will experience lift. This lift is obvious and can be calculated. The new weight of the load placed on the mass scale is recorded as the wind tunnel is being operated. The lift force experienced by the diamond shaped airfoil is the difference in weight of the load before and during the operation of the wind tunnel. The diamond shaped airfoil is removed from the test section and replaced with the circular arc airfoil. The circular arc airfoil is placed at angle 30° of attack and weight of the load connected to it is recorded before starting the wind tunnel. As the tunnel is being operated, the circular arc airfoil also experience lift. The new weight of the load on the mass scale is recorded as the wind tunnel is being operated. The lift force experienced by the circular arc airfoil is the difference in weight of the load before and during the operation of the wind tunnel.

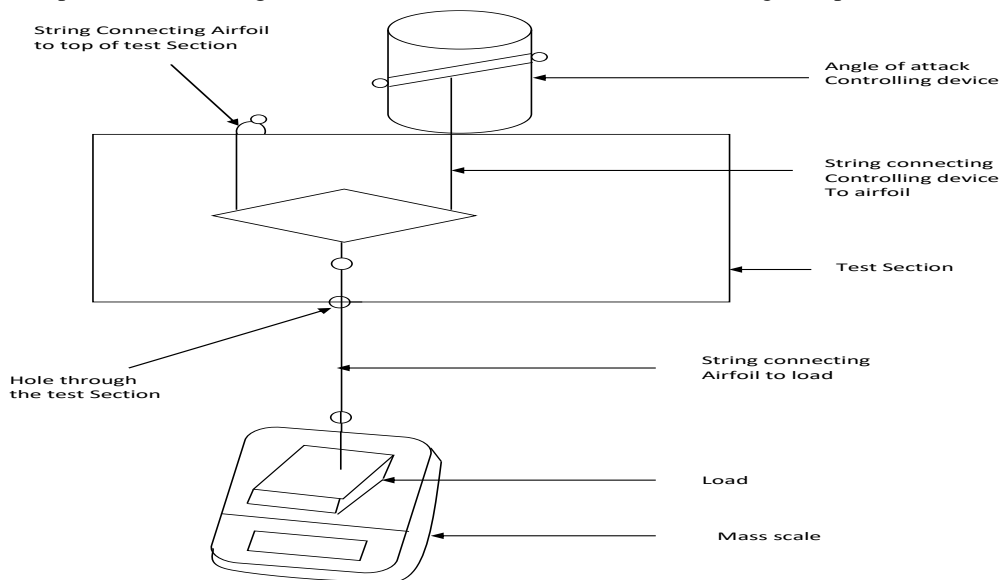


Figure 4: A sketch of diamond shaped airfoil connected to controlling device and load

The aircraft that is proposed to use this diamond shaped airfoil has the same data as that of a real aircraft named Executive aircraft (Cessna Citation 3).

The table of data for the Executive aircraft (Cessna Citation 3) was obtained as proposed by (Anderson, 2001) and is given as table 1.

Table 1: Data for the Executive aircraft (Cessna Citation 3)

Weight of aircraft (W)	140000 N
Wing area (A)	28m ²
Altitude(h)	13000m
Chord(c)	1m
Wing span (b)	28m

Since the Executive aircraft (Cessna Citation 3) has a wing designed from flat plate airfoil and not a diamond shaped airfoil, the thought of using a wing designed from diamond shaped airfoil arises. A diamond shaped airfoil must have thickness (t) and half wedge angle (δ_w). At supersonic speeds, airfoils with 3 to 5% thickness ratio are used. Furthermore,

the thickness ratio of an airfoil is a parameter which is usually specified. The diamond shaped airfoil is symmetrical when viewed from the side and is applicable for supersonic aircraft. The table of data of the diamond shaped airfoil that was analyzed in this research is given as table 2.

Table 2: Data for the diamond shaped airfoil

Weight of aircraft (W)	140000 N
Wing area (A)	28m ²
Altitude(h)	13000m
Chord(c)	1m
Wing span (b)	28m
Thickness (t)	0.05m
Half wedge angle (δ_w)	3°

2.5 Temperature, Pressure and Density at a given Altitude

Using the data in table 3 together with these equations; (17, 18 and 19), the temperature (T), pressure (P) and density (ρ) at a given altitude (h) were calculated and values are 203.65 K, 16355.6 N/m² and 0.2797 Kg/m³ respectively.

Table 3: Data for analysis

T _o	288.15 K
P _o	101325 N/m ²
L	0.0065 K/m
H	13000 m
G	9.806 m/s ²
M	0.02896 Kg/mol
R	8.3145 J/mol. K

2.6 Linear Theory Calculations for Diamond Shaped Airfoil



The diamond shaped airfoil was analyzed at different Mach number (Ma) ranging from Ma = 1.4 to Ma = 2.8. Using the data in table 4 (note; T_∞ , P_∞ and ρ_∞ are data obtained in section 2.5) together with equations (6 - 14), the different parameters such as; dynamic pressure (q_∞) at free stream condition (13000m altitude), lift coefficient (C_L), angle of attack (α), drag coefficient (C_D), the lift to drag ratio, $\frac{C_L}{C_D}$, deflection angle at surface 1(θ_1), coefficient of pressure at surface 1(C_{p1}), pressure at surface 1(P_1), temperature at

surface 1(T_1), deflection angle at surface 2(θ_2), coefficient of pressure at surface 2(C_{p2}), pressure at surface 2(P_2), temperature at surface 2(T_2), deflection angle at surface 3(θ_3), coefficient of pressure at surface 3(C_{p3}), pressure at surface 3(P_3), temperature at surface 3(T_3), deflection angle at surface 4(θ_4), coefficient of pressure at surface 4(C_{p4}), pressure at surface 4(P_4) and temperature at surface 4(T_4) were calculated and the data obtained for Mach numbers ranging from $M_\infty = 1.4$ to $M_\infty = 2.8$ are presented in table 7.

Table 4: Data used in my analysis of the diamond shaped airfoil

T_∞	203.65 K
P_∞	16355.6 N/m ²
ρ_∞	0.2797 Kg/m ³
M_∞	1.4
γ_{air}	1.4
R_S	287.058J/KgK

2.7 Linear theory Software for Airfoil

Linear theory equations were used to analyze the diamond shaped airfoil. The equations involve tedious numerical computation. The linear theory software was developed to eliminate the tedious numerical computation of linear theory equations which are used for theoretical analysis of airfoils. The linear theory software for airfoil was developed using

Microsoft visual basic.net 2010. The linear theory software for airfoil can compute the value of temperature, pressure and density at any given height and display the results, See figure 12. The linear theory software can also compute all parameters which are expressed in linear theory equations (6 - 14) and display the results (see figure 13). The linear theory software also shows the list of symbols with their respective meaning (see figure 14).

3. RESULTS AND DISCUSSION

The mass of diamond shaped airfoil; circular arc airfoil and load are 7.1g, 9.6g and 3.0g respectively. The diamond shaped airfoil and circular arc airfoil

are placed at angle 30° to airflow. The results are given in table 5 and table 6 for first and second reading respectively.

Table 5: First reading Table of data from mass scale at 30° angle of attack

	Angle of attack(α)	Weight of load(N) before testing	Weight of load(N) during testing	Lift force(N)
Diamond shaped airfoil	30°	30	19	11
Circular arc airfoil	30°	30	24	6

Table 6: Second reading Table of data from mass scale at 30° angle of attack

	Angle of attack(α)	Weight of Load(N) before testing	Weight of load (N) during testing	Lift force(N)
Diamond shaped airfoil	30°	30	20	10
Circular arc airfoil	30°	30	25	5

Table 7: Linear Theory Results for Diamond Shaped Airfoil

Mach	1.4	1.6	1.8	2.0	2.2	2.4	2.6	2.8
------	-----	-----	-----	-----	-----	-----	-----	-----

Number								
q_∞	22433.69	29301.14	37084.26	45783.03	55397.47	65927.57	77373.33	89734.75
C_L	0.22288	0.17064	0.13483	0.10921	0.09026	0.07584	0.06462	0.05572
α (degree)	3.1	3.0	2.9	2.7	2.5	2.4	2.2	2.1
C_D	0.02237	0.01710	0.01348	0.01094	0.00909	0.00772	0.00667	0.00585
C_L/C_D	9.96	9.98	10	9.98	9.93	9.82	9.69	9.52
θ_1	-0.26295^0	-0.1879^0	-0.0258^0	0.1553^0	0.3311^0	0.4944^0	0.6433^0	0.7774^0
C_{P_1}	-0.009369	-0.005252	-0.000601	0.003129	0.005899	0.007911	0.009358	0.01038
P_1	16145.41	16201.70	16333.30	16498.86	16682.40	16877.15	17079.66	17287.05
T_1	202.90	203.10	203.57	204.16	204.80	205.48	206.19	206.90
θ_2	-5.9918^0	-5.9167^0	-5.7546^0	-5.5736^0	-5.3977^0	-5.2344^0	-5.0855^0	-4.9514^0
C_{P_2}	-0.21349	-0.16538	-0.13423	-0.11234	-0.09616	-0.08376	-0.07398	-0.06609
P_2	11566.23	11509.78	11377.78	11212.33	11028.58	10833.51	10631.52	10425.03
T_2	184.46	184.20	183.59	182.83	181.96	181.04	180.06	179.06
θ_3	5.9918^0	5.9167^0	5.7546^0	5.5736^0	5.3977^0	5.2344^0	5.0855^0	4.9514^0
C_{P_3}	0.21349	0.16538	0.13423	0.11234	0.09616	0.08376	0.07398	0.06609
P_3	21144.97	21201.42	21333.42	21498.87	21682.62	21877.69	22079.68	22286.17
T_3	219.16	219.32	219.71	220.20	220.73	221.30	221.88	222.47
θ_4	0.26295^0	0.1879^0	0.0258^0	-0.1553^0	-0.3311^0	-0.4944^0	-0.6433^0	-0.7774^0
C_{P_4}	0.009369	0.005252	0.000601	-0.003129	-0.005899	-0.007911	-0.009358	-0.01038
P_4	16565.79	16509.50	16377.9	16212.34	16028.8	15834.05	15631.54	15424.15
T_4	204.39	204.20	203.73	203.14	202.48	201.77	201.03	200.27

The result from table 5 and table 6 showed that at angle 30° of attack, the diamond shaped airfoil produced a lift force of 11N and 10N respectively. The result from table 5 and table 6 showed that at angle 30° of attack, the circular arc airfoil produced a lift force of 6N and 5N respectively. This result shows that the diamond shaped airfoil produced

better lift force than the circular arc airfoil. The data for coefficient of pressures which was listed in table 7 was plotted to show the pressure distribution along the upper and lower surfaces of the diamond shaped airfoil. The result in figures 5 and 6 were extracted from table 7 for Mach number $M_\infty = 1.8$ for analysis because at Mach number $M_\infty = 1.8$, the lift to drag ratio was recorded as the maximum value.

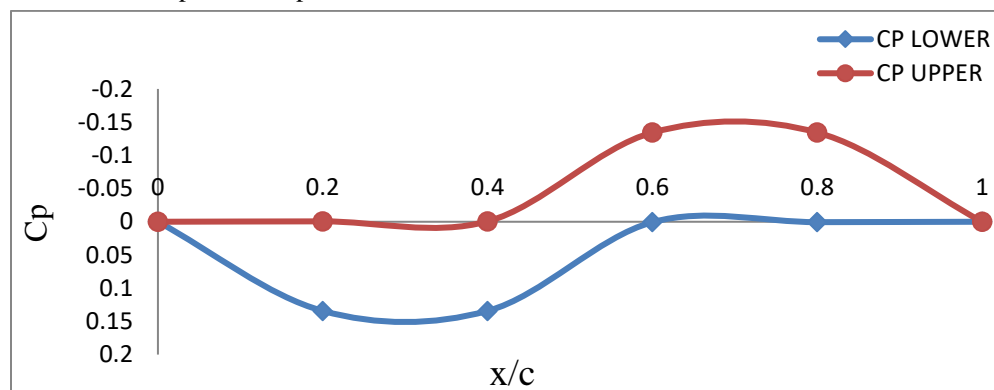


Figure 5: Pressure distribution for diamond shaped airfoil

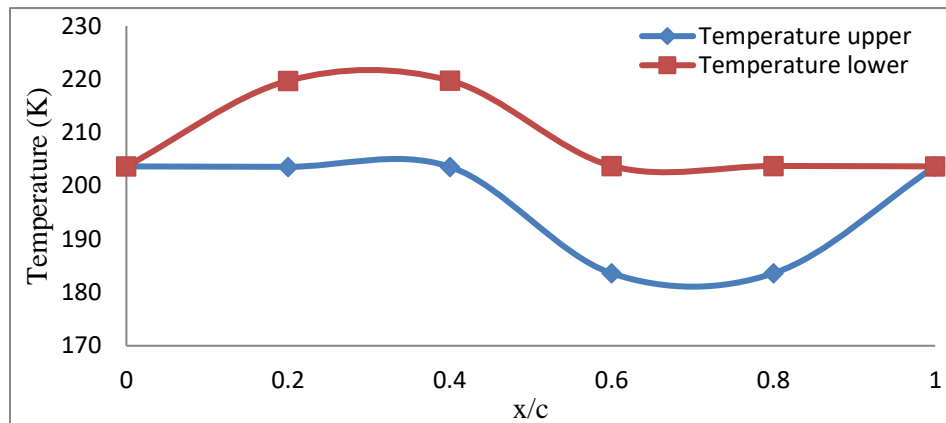


Figure 6: Temperature distribution for diamond shaped airfoil

From figure 5, it is obvious that Pressures are uniformly distributed on the surfaces of the diamond shaped airfoil. Maximum coefficient of pressure C_p was found on surface 3 of the diamond shaped airfoil with value of +0.15. Minimum coefficient of pressure C_p was found on surface 2 of the diamond shaped airfoil with value of -0.15. Bernoulli's equation is a method of showing that there is a lower pressure above the wing than below. Bernoulli equation shows that because the velocity of the fluid below the wing is lower than the velocity of the fluid above the wing, the pressure below the wing is higher than the pressure above the wing (Munson et al, 2005). The physical significance of Bernoulli's equation shows that when the velocity increases, the pressure decreases and when the velocity decreases, the pressure increases (Munson et al, 2005). From figure 5, it is shown that the pressure below the wing is

higher than the pressure above the wing. This pressure difference results in an upward lifting force on the wing, allowing the airplane to be lifted up. In reality, it is expected that the pressure below the wing should be higher than the pressure above. Since the air above the wing is moving faster, the airfoil lowers the air pressure, resulting in a lower pressure above and a higher pressure below, thereby creating lift.

Figure 6 shows temperatures on different surfaces of the diamond shaped airfoil. Maximum temperature was found on surface 3 of the diamond shaped airfoil with value of 219.71K. Minimum temperature was found on surface 2 of the diamond shaped airfoil with value of 183.59K. Variations of lift coefficient, C_L , and drag coefficient, C_D , with Mach numbers ranging from $M_\infty=1.4$ to $M_\infty=2.8$ were plotted on the same graph. This is shown in figure 7.

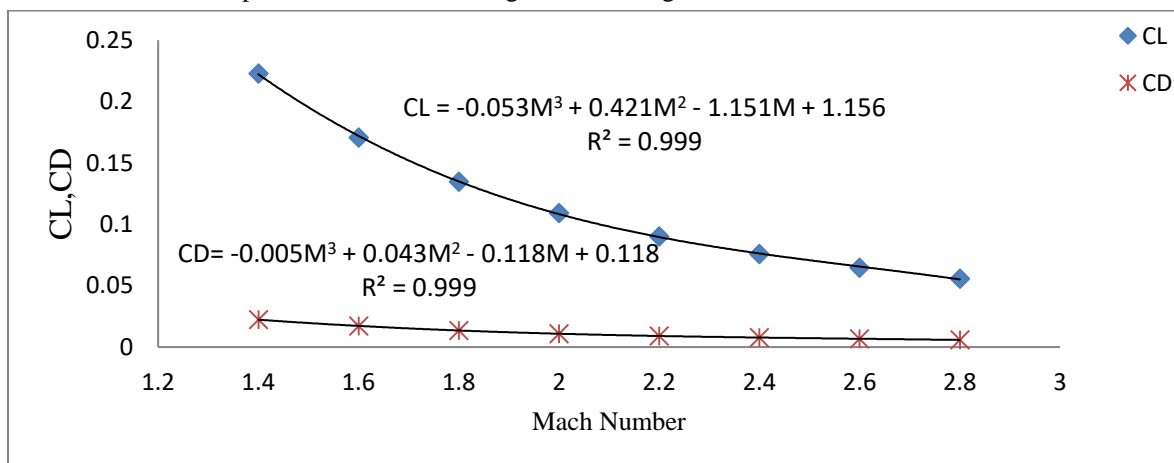


Figure 7: Variations of C_L and C_D with Mach number

From figure 7, it is obvious that values of lift coefficient C_L decrease as Mach number increases. At



the smallest Mach number, the lift coefficient is maximal. Since Mach number is related to the flight velocity (which is equivalent to the fluid velocity) from equation (4), therefore lift coefficient is maximal when flight velocity is the smallest. In real sense, this means that the lowest possible velocity at which the airplane can maintain steady level flight is the stalling velocity, V_{stall} ; it is dictated by the value of maximum lift coefficient. Also, it is obvious that values of drag coefficient, C_D decrease as Mach

number increases. The drag coefficient is maximal when Mach number is the smallest. Since Mach number is related to the flight velocity (which is equivalent to the fluid velocity) from equation (4), therefore drag coefficient is maximal when flight velocity is the smallest. At low Mach number, lift and drag are high. This result looks similar to a typical graph showing variations of lift coefficient and drag coefficient with Mach number as shown in figure 8.

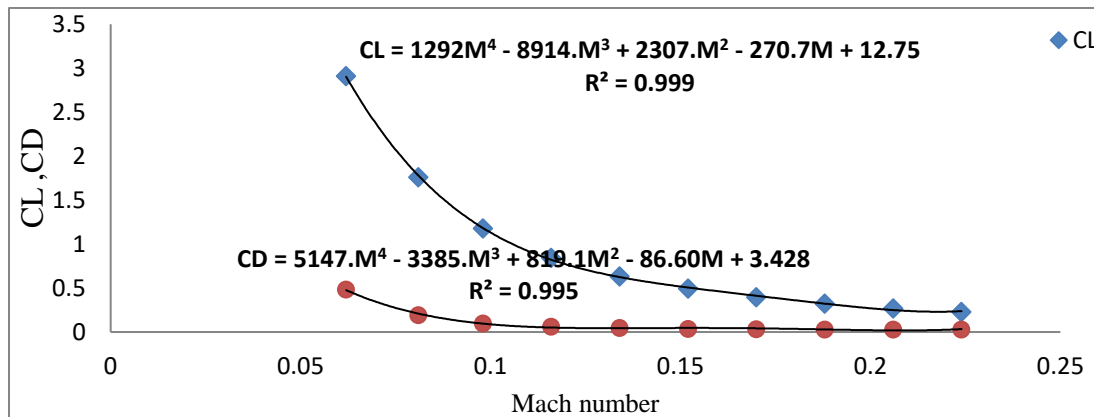


Figure 8: A typical graph showing variation of lift coefficient and drag coefficient with Mach number (Anderson, 2001).

Because lift and drag are both aerodynamic forces, the ratio of lift to drag (L/D ratio) is an indication of the aerodynamic efficiency of the airplane. As shown in equation (10), the L/D ratio is also equal to the

ratio of the lift and drag coefficients (C_L/C_D). Variation of lift to drag ratio (C_L/C_D) with Mach numbers ranging from $M_\infty=1.4$ to $M_\infty=2.8$ are presented in figure 9.

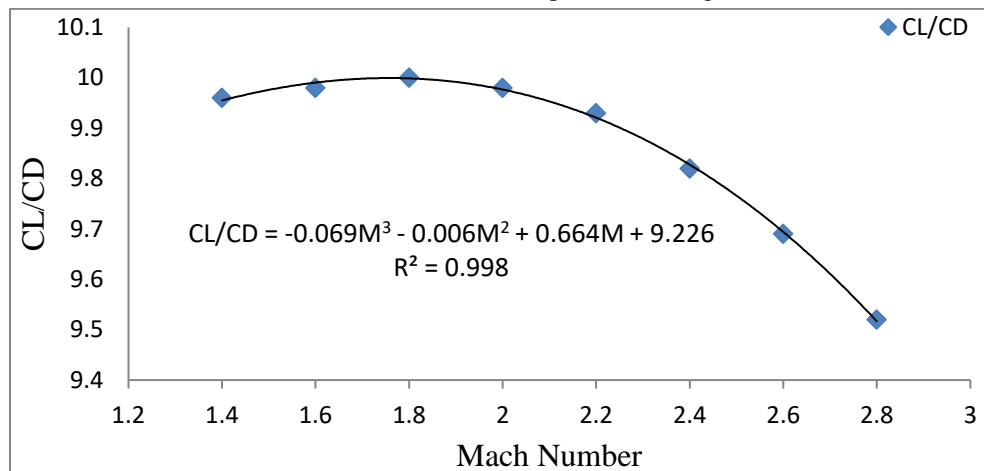


Figure 9: Variation of lift to drag ratio with Mach number

From figure 9, as Mach number increases from a low value, lift to drag ratio first increases, then reaches a maximum value of 10 at a Mach number of 1.8 and then decreases. This means that since lift to drag ratio

is a true measure of the aerodynamic efficiency of the body shape, the diamond shaped airfoil is most aerodynamically efficient at maximum lift to drag ratio of 10. This result looks similar to a typical graph

showing variation of lift to drag ratio with Mach number as shown in figure 10.

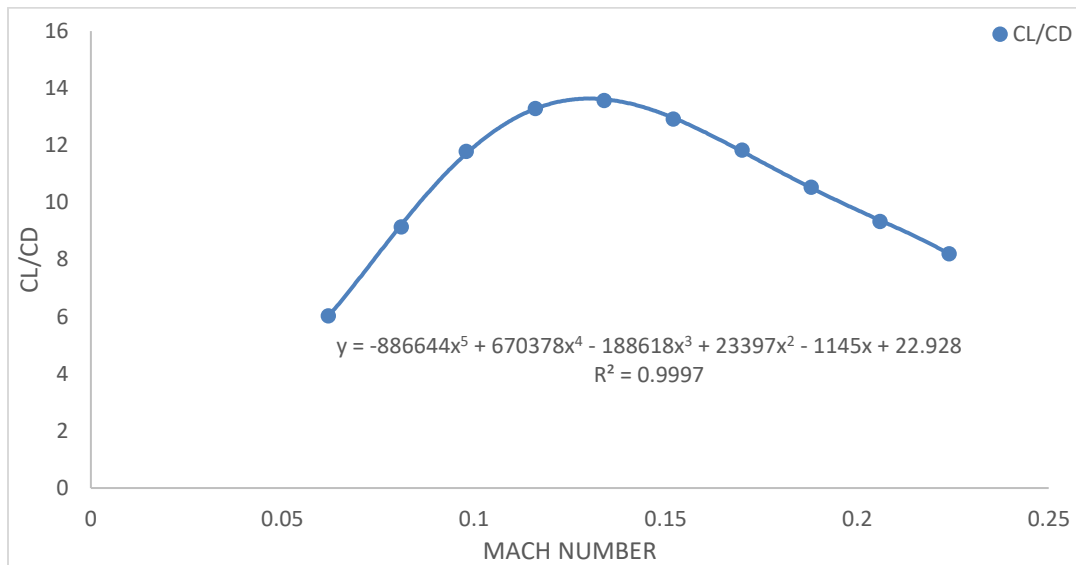


Figure 10: A typical graph showing variation of lift to drag ratio with Mach number (Anderson, 2001)

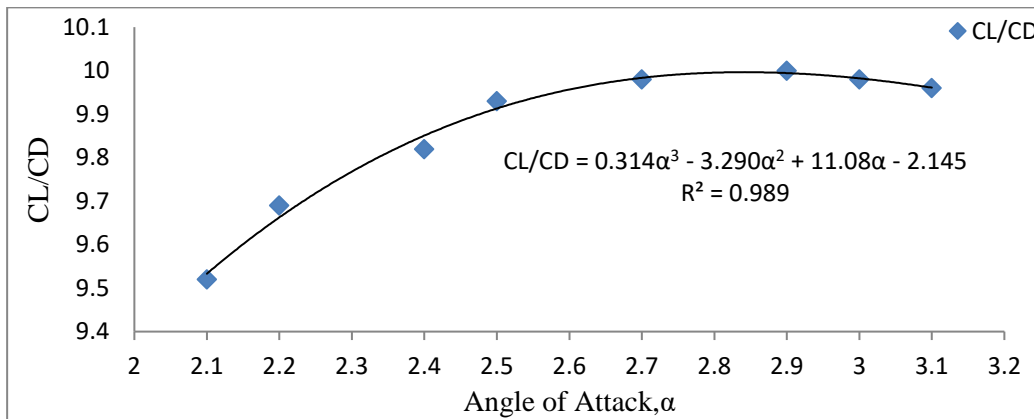


Figure 11: Variation of lift to drag ratio, (C_L/C_D) .with angle of attack, α .

From figure 11, it is obvious that as the angle of attack increases, the lift to drag ratio also increases, then reaches a maximum value of 10 at an angle of attack ($\alpha = 2.9^\circ$) and then decreases with a further increase in angle of attack. The physical meaning of this is that if the airplane is operated in steady flight

at maximum lift to drag ratio, L/D_{max} , the total drag is at a minimum. Any angle of attack lower or higher than the angle of attack for maximum lift to drag ratio, L/D_{max} , reduces the lift to drag ratio, L/D , and consequently increases the total drag for a given airplane's lift.

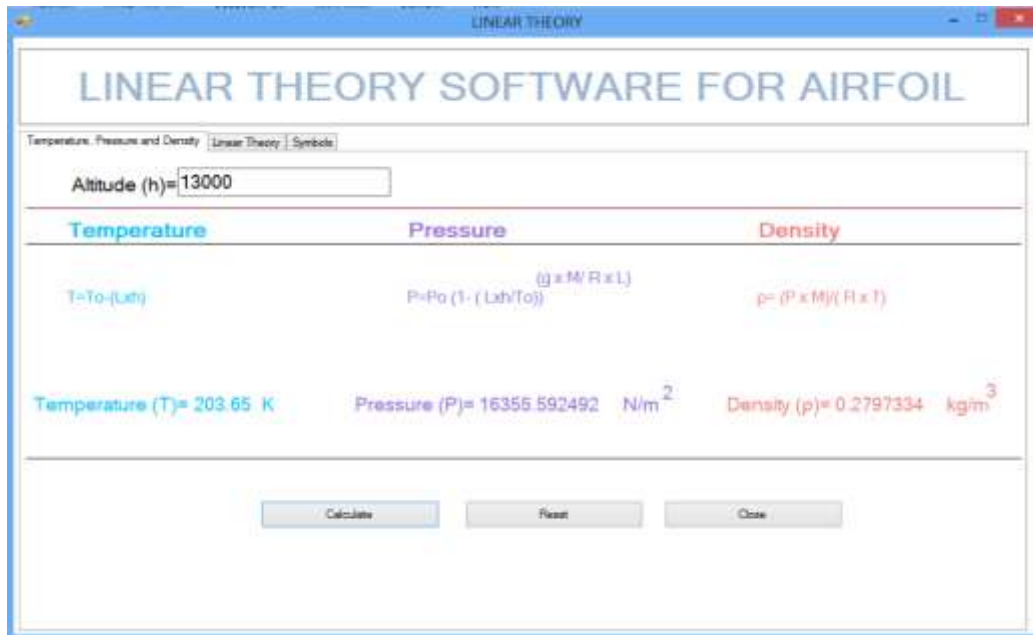


Figure 12: Acquisition of pressure, temperature and density data from linear theory software at a given altitude, h

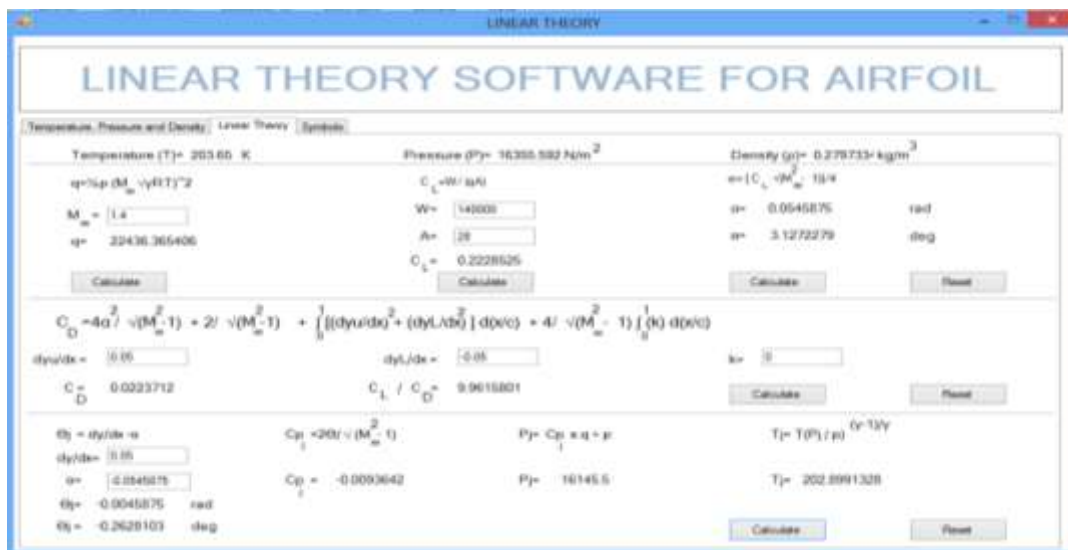


Figure 13: Linear theory software results for Mach number of 1.4 at surface 1



Symbol	Description	Symbol	Description
T	Temperature at altitude h (K)	A	Wing Area (m ²)
T ₀	Standard Temperature	α	Angle of attack
L	Lapse rate (km)	C _D	Drag Coefficient
h	Altitude (m)	δ _u	Upper thickness ratio
P	Pressure at altitude h (N/m ²)	δ _l	Lower Thickness ratio
P ₀	Standard atmospheric pressure (N/m ²)	θ ₁	Deflection angle at surface
S	Oxidational acceleration (m/s ²)	C _{p1}	Coefficient pressure at surface
M	Molar ratio (kg/mol)	T ₁	Temperature at surface
R	Universal gas constant (J/molK)	C _L / C _D	Lift to drag ratio
Mach	Free Stream Mach number		
ρ _∞	Free Stream dynamic pressure (N/m ²)		
P _∞	Free stream density (kg/m ³)		
h	Specific heat of air		
C _L	Lift coefficient		
W	Weight (N)		

Figure 14: List of symbols for linear theory software for airfoil

4. CONCLUSION

It is therefore concluded that the diamond shaped airfoil produced better lift force than the circular arc airfoil. The diamond shaped airfoil can be used in place of other airfoils (e.g. circular arc airfoil) because it has no camber and curved surfaces and therefore is easier to construct. The diamond shaped airfoil is therefore recommended for the design of new aircraft's wing. The performance of the diamond shaped airfoil was analyzed using linear theory. The diamond shaped airfoil was selected for study because it is a symmetrical airfoil which has no camber or curved surfaces and is easier to construct. The diamond shaped airfoil provides good lift to drag ratio as found in this research and is easier to construct due to the absence of camber and curved surfaces. Maximum pressure and temperature were found on surface 3 of the diamond shaped airfoil with

values of 21333.42N/m² and 219.71K respectively while minimum pressure and temperature were found on surface 2 of the diamond shaped airfoil with values of 11377.78N/m² and 183.59K respectively at Mach number of 1.8 which gave the maximum lift to drag ratio of 10. By Bernoulli's Theorem, due to the pressure difference produced between the upper and lower surfaces of the wing, the lift is produced which makes the aircraft to fly. A lift to drag ratio of 10 is high enough as compared for lift to drag ratios of conventional aircraft. Therefore, it is concluded that the diamond shaped airfoil can be used for aircraft's wing because it gives high lift to drag ratio and therefore is capable of producing high lift force which makes the plane to fly in the air. The diamond shape airfoil can be used for supersonic aircrafts and fighter jets like the F-117A jet.

REFERENCES

1. Anderson (2001). Fundamentals of Aerodynamics, McGraw-Hill Companies, Inc. New York, 3rd edition, 437- 650.
2. Auld D. J. and Srinivas K. (2010). Aerodynamics for students. Aerospace, Mechanical and Mechatronic Engineering, University of Sydney, http://www-mdp.eng.cam.ac.uk/web/library/enginfo/aerothermal_dvd_only/aero/contents.html
3. Bertin J. J., Cummings R. M. (2009). Aerodynamics for Engineers. Pearson Prentice Hall Ed. (5th Ed.).
4. Bruschi G., Nishioka T., Tsang K., Wang R. (2003). Wind tunnel experiment, Clark Y-14 airfoil Analysis.
5. http://209.141.57.135/projects/docs/mae171_a/wind_tunnel_experiment.pdf
6. Cavcar M. (2012). Pressure distribution around an airfoil, March 5, 2012 http://home.anadolu.edu.tr/~mcavcar/hyo30_1/14_PressureDistribution.pdf
7. Douglas J. F. (2000). Fluid Mechanics. Pitman Publishing New Zealand Ltd, Wellington, 329 -340.

-
8. Houghton, E. L., Carpenter, P. W. (2003). Aerodynamics for Engineering Students. Butterworth Heinmann.
 9. Karabelas S. J. and Markatos N. C. (2008). Water Vapour Condensation in Forced Convection Flow over an Airfoil, Aerospace Science and Technology, 12(2): 150 - 158.
 10. Munson R. B., Donald F. Y., Theodore H. O. (2005). Fundamentals of Fluid Mechanics, 5th edition.
 11. PrabhakarRao P. and Sampath S. V. (2014). CFD Analysis on Airfoil at High Angles of Attack. International Journal of Engineering Research, 3(7): 430 - 4343.
 12. Salem B. G. and Ibrahim K. M. (2004). Measurement of pressure distribution over a cambered airfoil.